

Enhancement of photovoltaic performance of quasi-solid state dye sensitized solar cell with dispersion of a hole conducting agent

S. RANI¹, P.K. SHISHODIA², R.M. MEHRA^{1*}

¹Department of Electronic Science, University of Delhi, South Campus, New Delhi – 110 021, India

²Department of Physics & Electronics, Zakir Husain College,
University of Delhi, New Delhi – 110 002, India

The presence of a hole conducting agent in a quasi-solid state dye sensitized solar cell (DSSC) may improve cell parameters. The paper reports on the photovoltaic properties of two types of cells, one containing a layer of CuI on a dye coated ZnO electrode (cell A) and the other with CuI dispersed in a gel electrolyte (cell B). The cell A generated a short circuit current density of $7.45 \text{ mA}\cdot\text{cm}^{-2}$, an open-circuit voltage of 0.56 V, a fill factor of 0.54 and an overall power conversion efficiency of 2.26% under $100 \text{ mW}\cdot\text{cm}^{-2}$ (air mass: 1.5). In cell B, an enhancement in its performance was observed. The cell showed 2.67% efficiency with a short circuit current density of $8.75 \text{ mA}\cdot\text{cm}^{-2}$, an open-circuit voltage of 0.59 V and a fill factor of 0.52. The increase in the performance is attributed to the improvement in the hole transport in the electrolyte. The efficiency of cell B was further increased to 3.38% by introducing a compact layer of ZnO 106 nm thick.

Keywords: ZnO DSSC; layered CuI; dispersed CuI; ZnO compact layer

1. Introduction

Dye sensitized nanocrystalline solar cells have intensively been investigated, as they offer an attractive alternative to conventional p-n junction solar cells, because of their high efficiency, simple fabrication process and low production cost [1, 2]. In solid state versions, the electrolyte present in the pores of a mesoporous oxide film is replaced by a large band gap p-type semiconductor [3–6]. Light is absorbed by the dye adsorbed on the oxide surface. Upon excitation, the dye injects electrons into the conduction band of the oxide and is regenerated by injection of holes into the p-type conductor. A great advantage of such systems with regard to conventional p-n junctions is that only majority carriers are involved in the photoelectric conversion process.

*Corresponding author, e-mail: rammehra2003@yahoo.com

TiO₂ based quasi-solid state dye sensitized solar cell (DSSC) produce energy conversion efficiencies as high as ca. 11%, Typical DSSC are normally arranged in a sandwich configuration, that is the space between dye sensitized semiconductor (e.g., TiO₂) and counter electrodes is filled with an organic solution containing I⁻/I₃⁻ redox couple as a cell electrolyte. Problems such as leakage and solvent evaporation associated with liquid electrolyte results in lower long-term stability and a decrease in cell performance. Many efforts have been made to replace liquid electrolytes with solid state or quasi-solid state ones such as inorganic p-type semiconductors [7], organic hole conductors [8], polymer/polymer gels [9, 10] and other new materials [11, 12]. Inexpensive ZnO powder is expected to be an alternating wide bandgap semiconductor because of its many important physical properties, such as large exciton binding energy of 60 meV at room temperature and good electrical conductivity [13]. Recently we reported results on ZnO based quasi-solid state DSSC fabricated using the sol-gel derived ZnO powder [14].

Solid state cells comprising CuI as a p-type semiconductor, to conduct away the holes, exhibit low conversion efficiencies [15], compared with the liquid version due to the low conductivity of charge carriers in the electrolytes and incomplete penetration of the solid electrolyte in the voids of the porous electrode. Therefore, quasi-solid state cells have received much attention because they have higher conductivities and higher conversion efficiencies compared with solid state cells. There are a number of reports on the use of organic or inorganic fillers in gel electrolytes in order to increase the efficiency of quasi-solid state dye sensitized solar cells. For example, Wang et al. [16] obtained a quasi-solid state electrolyte by solidifying the ionic liquid (1-methyl-3-propylimidazolium iodide) electrolyte with fluorine polymer (poly(vinylidene fluoride-co-hexafluoropropyl-ene)), achieving 5.3% overall conversion efficiency of the cells. Usui et al. [17] found improved conversion efficiency by dispersing TiO₂ nanoparticles in a ionic gel electrolyte. Kubo et al. [18] studied a quasi-solid state electrolyte by mixing the gelator with low molecular weight ionic liquid and achieved a cell with the conversion efficiency of 5%. Wang et al. reported DSSC with an ionic gel electrolyte containing dispersed silica nanoparticles [19]. The dispersion of various agents such as CNT, TiO₂, carbon black and graphite in ionic gel electrolyte enables the use of nanoparticles as “gelators” to solidify ionic liquid-based electrolytes and also increase the photovoltaic output [17].

In this paper, the authors have studied the effect of dispersion of hole conducting materials such as CuI in gel electrolyte to increase the photovoltaic performance of ZnO based quasi-solid state dye sensitized solar cells. The solar cell containing CuI as a layer on dye coated ZnO electrode and CuI dispersed in gel electrolyte were formed. The purpose of this work is to investigate various technologies which affect the photovoltaic performance, such as the application of CuI in various forms (layer or dispersion) to collect holes. The effect of a ZnO compact layer on photovoltaic performance was also investigated.

2. Experimental

Preparation of the polymer gel electrolyte. The polymer gel electrolyte was synthesized as follows: 3.0 g of poly ethylene glycol (PEG MW₆₀₀₀), 0.03 g of tetra propyl ammonium iodide (TPAI), 0.003g of I₂, 0.15 g of ethylene carbonate (EC): propylene carbonate (PC) 1:1 in 25 cm³ acetonitrile were used. TPAI and I₂ were firstly dissolved in a binary organic solvent mixture containing EC and PC (1:1) Then PEG was added and the solution was heated at 75–80 °C under vigorous stirring until a viscous gel was obtained, followed by cooling to room temperature.

Dispersion of CuI in polymer gel electrolyte. A composite polymer gel electrolyte was formed by dispersing 0.3 cm³ of filtered acetonitrile solution of CuI (0.16 M) in the polymer gel electrolyte, prepared as above (0.9 cm³) at 60 °C under continuous stirring. A DSSC using the dispersed CuI polymer gel-electrolyte was fabricated by spreading the composite electrolyte on a dye coated ZnO electrode and then applying a counter electrode.

Preparation of ZnO electrode and treatment with the dye. Porous ZnO films, produced using nanocrystalline ZnO powder, were deposited on indium tin oxide (ITO) coated glass from the synthesized ZnO powder by the doctor blade technique [14]. Rose Bengal (RB) dye was used to sensitize the ZnO film. RB is an organic dye in the xanthene class. It absorbs a wide spectrum of solar energy and energetically matches the ZnO and iodine/iodide redox couple for DSSC application [20, 21]. Thus ZnO performs particularly well when sensitized with Rose Bengal [22]. Being an organic dye, there are no concerns about environmental damage, as it does not contain any noble metal, such as ruthenium. RB dye has been successfully used by several groups for DSSCs structures. It has high extinction coefficients and its molecular structure contains anchoring groups that can be adsorbed onto the oxide surface [23]. For the particular case of ZnO–RB (or other anionic xanthenes dyes), it is highly probable that the dye is directly bound to the surface of a zinc ion. Such bonding will not only make the adsorptivity high but also facilitate the electron injection process by a strong overlap between the electron molecular orbitals of the dye and those of the conduction band of the semiconductor [22]. The ZnO film was immersed in a 0.3 mM solution of Rose Bengal dye in ethanol for 24 h. To minimize the adsorption of impurities from moisture in the ambient air, the electrodes were dipped in the dye solution while they were still warm (ca. 80 °C). The dye covered electrodes were then rinsed with ethanol, to remove excess dye on the surface, and dried at room temperature.

Formation of CuI layer. A solution of CuI (0.16 M) was prepared by dissolving 0.3 g of CuI in 10 cm³ of moisture free acetonitrile. The dye coated ZnO electrode was placed on a hot plate (80–100 °C) and filtered (0.3 cm³) acetonitrile CuI solution was spread over the dye coated ZnO electrode.

Preparation of ZnO compact layer. The ZnO compact layer was prepared by the sol-gel technique. Sols were prepared by dissolving zinc acetate ($\text{Zn}(\text{CH}_3\text{COO})_2 \cdot 2\text{H}_2\text{O}$, 99.0% purity) in methanol to form 0.2 M solution. The mixture was stirred with an ultrasonic and magnetic stirrer at 25 °C for 120 min until a clear solution was formed. The sol prepared was found to be stable and transparent with no precipitate or turbidity. Monoethanolamine (MEA) was further added to the sol to achieve the pH of ca. 9. The modified sols were stirred ultrasonically for 60 min at room temperature. The sols were then kept for 48 h for aging in order to convert the sol into gel. The conductive glass substrate (ITO) was cleaned using acetone, methanol and distilled water in an ultrasonic bath. The ZnO film was spin coated on the substrate at a spinning speed of 3000 rpm for 20 s. The desired thickness of the ZnO compact layer was varied by repeatedly applying the appropriate number of coatings. The films were dried on a hot plate at 300 °C for 10 min in between each successive layer deposition. Since the boiling point of MEA and temperature of thermal decomposition of zinc acetate are 170 °C and 240 °C respectively [24], a preheat treatment temperature of 300 °C is sufficient for the complete evaporation of organics. The deposited ZnO compact layer films were annealed in air at 400 °C for 1 h. The thickness of the film was measured by the reflectance method.

Solar cell assembly. The assembled solar cells are: cell A: CuI in a layer form (ITO/ZnO/Rose Bengal/CuI layer/gel electrolyte/Pt), and cell B: CuI dispersed in a gel electrolyte (ITO/ZnO/Rose Bengal/dispersed CuI gel electrolyte/Pt). Pt sheet was used as a counter electrode. The active electrode area was typically 1 cm².

Characterization and J–V measurement. The crystalline nature of ZnO powder and ZnO electrode was determined by X-ray diffraction (XRD) using a Philips analytical Model No.-PW1830 with a CuK_α incident beam ($\lambda = 1.54 \text{ \AA}$). The presence of CuI on the ZnO surface and in gel electrolyte was confirmed by X-ray diffraction. The surface morphology of the ZnO electrode was analyzed by using a scanning electron microscope (SEM) (LEO 435 Vp, variable pressure scanning electron microscope, Cambridge UK). The absorbance of the ZnO electrode, sensitized with Rose Bengal dye was measured using a UV-VIS-NIR spectrophotometer (SolidSpec-3700, Shimadzu, Japan). The spectrophotometer was equipped with an integrating sphere which enabled recording the reflectance. The absorbance is obtained by transforming the diffused reflectance data using the Kubelka–Munk function.

The solar energy conversion efficiency ($J-V$) curve was measured by using a computerized digital Keithley source meter (Model 2400) and a tungsten halogen lamp as the light source. The lamp was calibrated close to AM1.5 SUN conditions from National Physical Laboratory (NPL, New Delhi). The IR radiation was attenuated using a water filter. A tungsten halogen lamp does not assure AM conditions since its source of light contains insufficiently small amounts of UV light. Therefore generally xenon arc lamps are used in solar simulators. Although in such a case the

absolute value of solar cell parameters would slightly differ from the actual one but this would not significantly affect the comparative study [25, 26].

Based on the J - V curve, the fill factor (FF) is defined as:

$$FF = \frac{I_{\max} V_{\max}}{I_{\text{sc}} V_{\text{oc}}}$$

where I_{\max} and V_{\max} are the photocurrent density and photovoltage for maximum power output (P_{\max}), I_{sc} and V_{oc} are the short-circuit current density and open circuit voltage, respectively. The overall energy conversion efficiency η is defined as:

$$\eta = \frac{I_{\text{sc}} V_{\text{oc}} FF}{P_{\text{in}}}$$

where P_{in} is the power of the incident light.

The incident photon-to-current density conversion efficiency (IPCE) gives the ratio between the number of generated charge carriers contributing to the photocurrent density and the number of incident photons, and is given by

$$\text{IPCE} = \frac{1240 j_{\text{sc}}}{\lambda P_{\text{in}}} \%$$

where j_{sc} [mA/cm^2] is the short circuit current density, P_{in} [mW/cm^2] is the light power density and λ [nm] is the wavelength. j_{sc} of the cells was determined from the J - V characteristics of the cells obtained at various wavelengths of light using narrow bandwidth (10–12 nm) interference filters (Vin Karola Instruments, USA). The intensity of the incident monochromatic radiation was kept constant and measured using an optical power meter (Model 1815-C, Newport USA).

3. Results and discussion

3.1. Structural characterization

Figure 1 shows a SEM image of synthesized ZnO powder. Microstructural homogeneities are visible in the morphology of ZnO powder. The diameter of ZnO particles is approximately 1 μm . Figure 2 shows the SEM micrograph of the ZnO film on ITO sintered at 400 $^{\circ}\text{C}$. The film is porous with a homogeneous distribution of particles, tightly packed with good connectivity between them.

Figure 3a shows the XRD pattern of synthesized ZnO powder. The powders showed their crystalline nature, with peaks corresponding to the (100), (002) and (101) planes. The preferred orientation corresponding to the (101) plane is observed for ZnO powder. The spacing values and relative intensities of the peak coincide with the JCPDS card No. 36-1451 for ZnO powder.

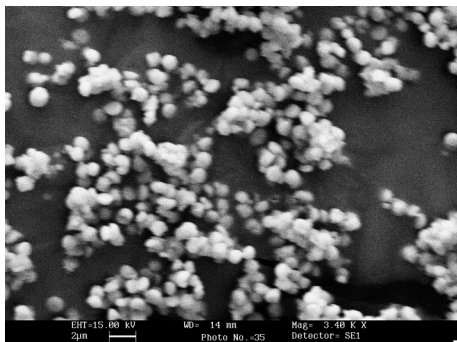


Fig. 1. SEM images of ZnO powder grown at pH = 9 in sol

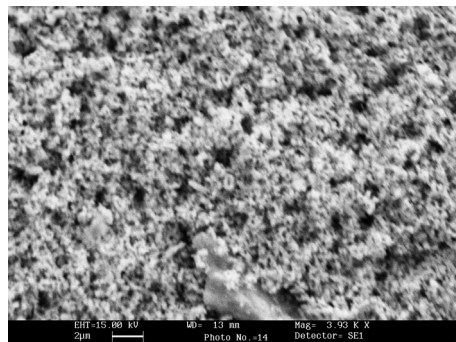


Fig. 2. SEM image of the ZnO film on ITO sintered at 400 °C

Crystallite size D was obtained from the full width at half maximum β of (101) peak using the Debye–Scherrer formula [27, 25]

$$D = \frac{0.94\lambda}{\beta \cos \theta}$$

where λ is the wavelength of CuK_α radiation and θ is the angle obtained from the 2θ value corresponding to the maximum intensity peak in the XRD pattern. The crystallite size of ZnO powder was found to be ca. 28 nm.

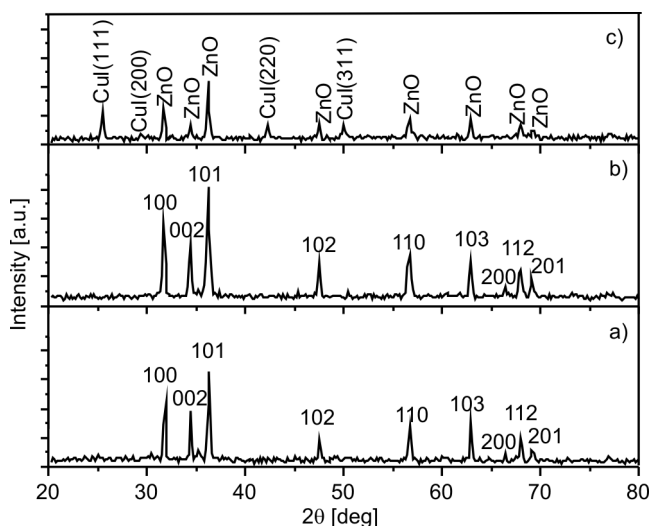


Fig. 3. XRD patterns of a synthesized ZnO powder (a), ZnO film on ITO (b), and after deposition of CuI layer on ZnO film (c)

Figure 3b shows the XRD pattern of ZnO films on ITO sintered at 400 °C. The film shows the polycrystalline nature with a preferred orientation corresponding to (101). Fig-

ure 3c shows the XRD pattern of ZnO electrode after deposition of CuI. It contains the peaks of both ZnO and CuI. CuI crystallizes in the zinc blende structure with γ -phase while the preferential orientation is the (111) direction.

To show the presence of CuI in gel electrolyte, films of gel electrolyte were deposited on Corning glass (7059) by the spin coating unit. Figure 4 shows the XRD pattern of the films before and after dispersion of CuI in gel electrolyte. It shows the presence of CuI in gel electrolyte with the preferential orientation in (111) direction.

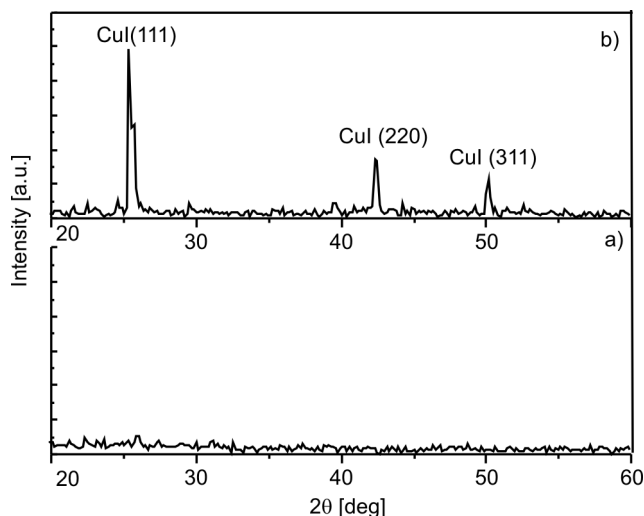


Fig. 4. XRD patterns of a gel electrolyte (a) and dispersed CuI (b) in gel electrolyte

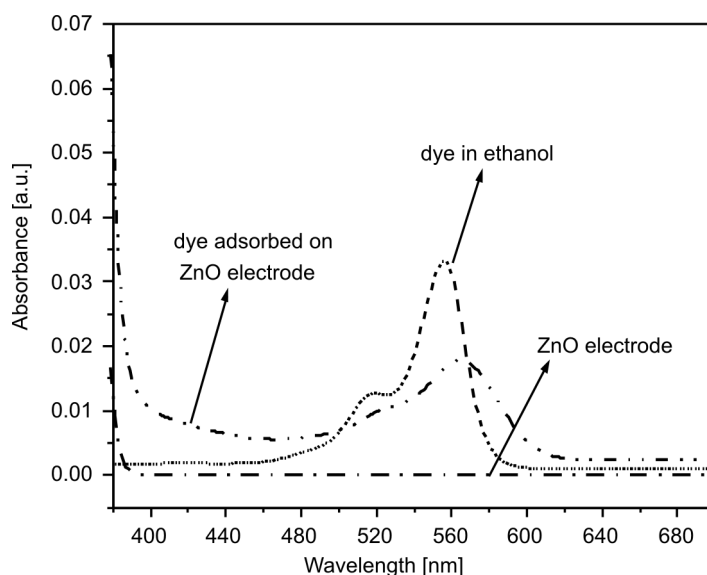


Fig. 5. UV-VIS absorption spectra of the Rose Bengal dye on ZnO surface

The absorbance of a ZnO electrode with and without dye is shown in Fig. 5. The absorption spectrum shows that the dye absorbs visible light in the 400–670 nm range with the maximum absorption at 564 nm. A broader absorption spectrum of the dye on the porous layer of ZnO is observed as compared with that in ethanol.

3.2. Effect of dispersion of CuI particles in gel electrolyte (J – V measurement)

Figure 6 shows the J – V characteristics of cells A and B. The J – V characteristic of a solar cell without CuI is also shown in the figure. The obtained solar cell parameters are given in Table 1. The cell made without the use of CuI was characterized by $J_{sc} = 6.21 \text{ mA}$, $V_{oc} = 0.58$ and $\eta = 1.92\%$. Enhancement in the photovoltaic performance is observed when CuI was used in the cell structure, and the increment in performance depends on the fabrication technique (layer or dispersed form). The J_{sc} , V_{oc} , FF , and η for the cell A having CuI in a layer form were found to be $7.45 \text{ mA}\cdot\text{cm}^{-2}$, 0.56 V , 0.54 , and 2.26% respectively while the solar cell B with CuI in a dispersed form by $J_{sc} = 8.75 \text{ mA}\cdot\text{cm}^{-2}$, $V_{oc} = 0.59 \text{ V}$, $FF = 0.52$ and $\eta = 2.67\%$. It may be mentioned that various cells were fabricated under identical conditions. There was no significant change in the J – V characteristics, including the value of V_{oc} and J_{sc} .

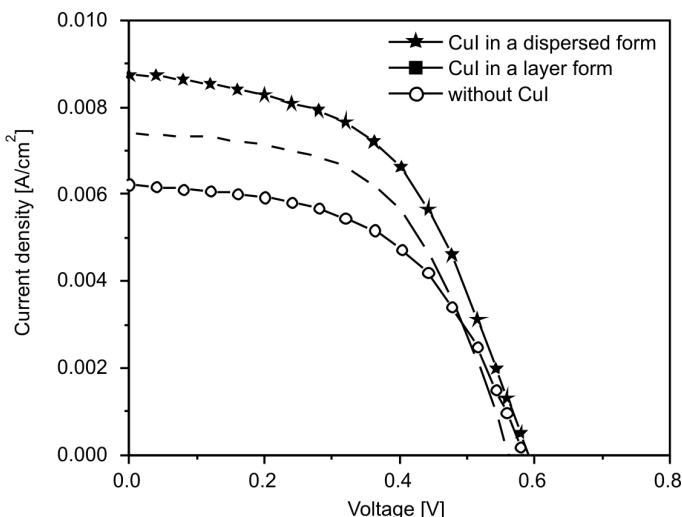


Fig. 6. J – V characteristics of solar cells showing the effect of addition of CuI on photovoltaic performance

Table 1. Photovoltaic parameters of DSSC employing CuI in various forms

Solar cell	J_{sc} [mA/cm ²]	V_{oc} [V]	FF	η [%]
Without CuI	6.21	0.58	0.53	1.92
CuI in a layer form	7.45	0.56	0.54	2.26
CuI in a dispersed form	8.75	0.59	0.52	2.67

Figure 7 shows the influence of CuI concentration on the performance of DSSC. When 0.3 cm^3 of CuI (0.16 M) was added to 0.9 cm^3 of gel electrolyte (the ratio of CuI to gel electrolyte was 1/3), V_{oc} , J_{sc} and η were found to have maximum values. V_{oc} decreases as the ratio of CuI/gel increases. J_{sc} and η also showed the same trend.

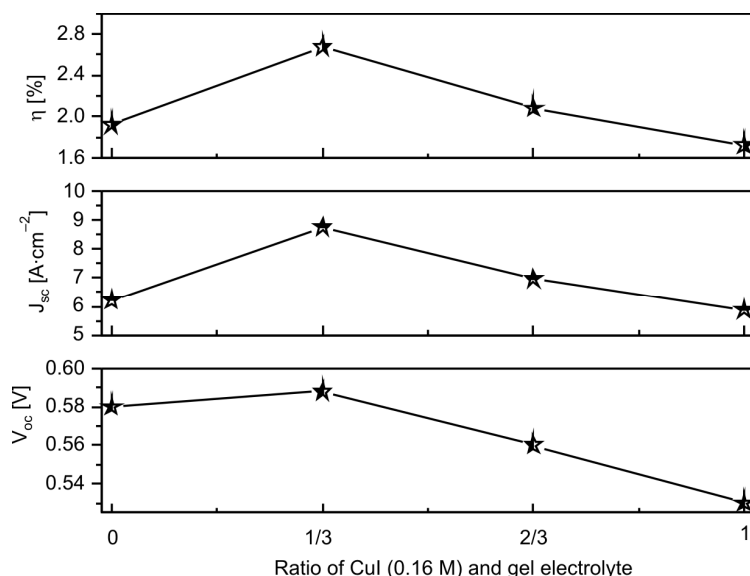


Fig. 7. Influence of the CuI concentration in gel electrolyte on the performance of DSSC

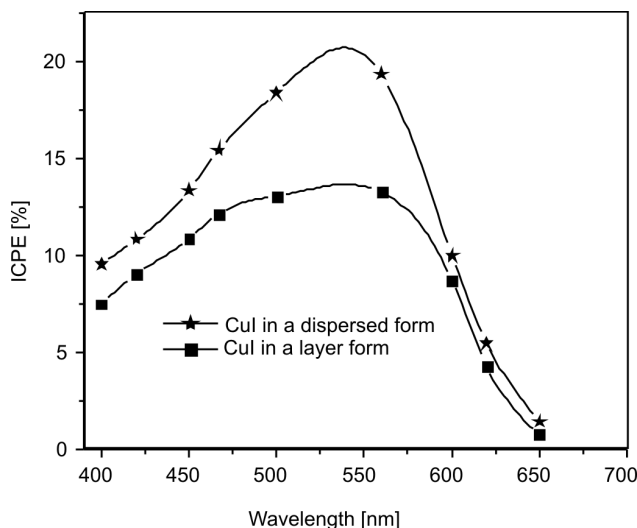


Fig. 8. Effect of layered and dispersed CuI on IPCE of a solar cell

Figure 8 shows the IPCE of the two solar cells A and B. Cells A and B show a maximum IPCE of ca. 14% and 20% at 564 nm, respectively. The peak in IPCE spectra

at ca. 564 nm is close to the observed peak in the absorbance of the ZnO electrode sensitized with RB dye. One of the recent papers also reports that the sensitization of TiO₂ layer with RB causes a widening of the spectral response covering the visible region, and results in high value of IPCE [28]. In the present case, also this could be the reason for a high value of IPCE in the range of 400–470 and 600–650 nm.

The IPCE is expressed in terms of the light harvesting efficiency of the dye (LHE), the quantum yield of electron injection (η_{inj}) and the efficiency of collecting the injected electrons (η_{cc}) at the transparent back contact, as described in [29]:

$$IPCE(\lambda) = LHE(\lambda)\eta_{inj}\eta_{cc}$$

A high IPCE is the result of either efficient light harvesting by the dye, efficient charge injection into ZnO, or efficient collection of injected electrons.

In the present case, only the conducting property of the electrolyte has been modified. The observed increase in the value of IPCE with the dispersion of CuI in TPAI+PEG gel electrolyte indicates an efficient collection of holes at the back contact.

3.3. Mechanism for achieving higher photocurrent density

Several workers have attempted to improve the properties of electrolytes by adding nanofillers such as TiO₂ particles, MWCNT and carbon black [17, 30–32]. It has been shown that the addition of nano fillers in the ionic liquid electrolyte reduces the resistance of the electrolyte and increases the redox couple mobility. Recently, Chen et al. [33] used CuI as an additive in an ionic liquid electrolyte (HMImI). It has been shown that CuI dissolves in HMImI and exists as Cu⁺ and I[−] in the electrolyte. Cu⁺ ions are adsorbed on TiO₂ which results in the increase in I_{sc} and the decrease in V_{oc} .

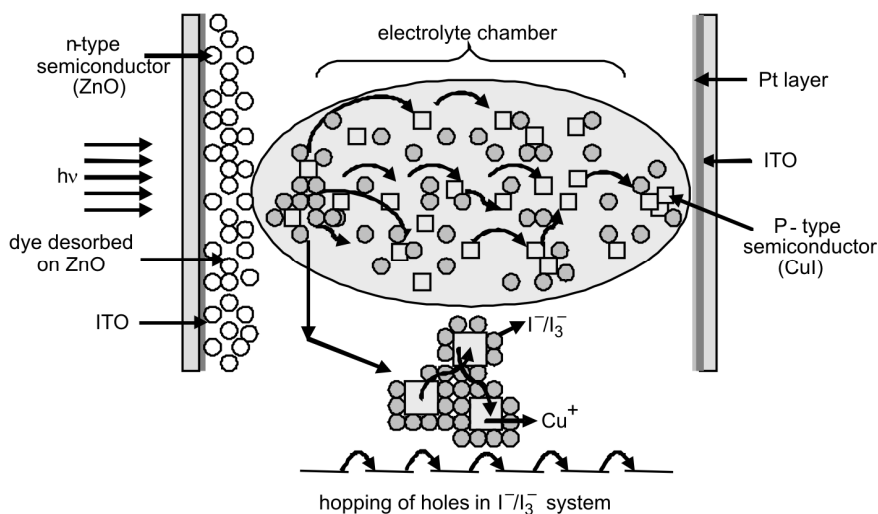


Fig. 9. Mechanism of hole transport in dispersed CuI gel electrolyte

In the present case (Cell B), the dispersion of CuI in the gel electrolyte (TPAI + PEG) resulted in the increase in I_{sc} without affecting V_{oc} unlike the values obtained for Cell A which had a layer of CuI on the ZnO electrode. It is assumed that the dispersed CuI dissociates into Cu^+ and I^- ions in the gel electrolyte and forms $Cu^+/I^-/I_3^-$ complexes, thereby introducing local ordering of the redox couple as shown in Fig. 9. This local ordering facilitates the hole conduction at back electrode which results in the higher conversion efficiency of the solar cell B. The efficiency of DSSC increased from 1.92 to 2.67% (Table 1) by the introduction of hole conducting agent CuI to the gel electrolyte (TPAI + PEG). Figure 9 illustrates the hopping of positive charges (holes) between I^-/I_3^- and Cu^+ .

3.4. Effect of ZnO compact layer on photovoltaic performance

The photovoltaic properties of fabricated solar cell B was further improved by applying ZnO compact layer on a conductive glass substrate. The introduction of a thin, ZnO compact layer in a dye sensitized solar cell can prevent a short circuit in the cell and therefore may inhibit the back transfer of electrons by blocking direct contact between the electrolyte and the conductive glass substrate [6]. Figure 10 shows the photocurrent density–voltage characteristics of solar cells, and the cell parameters are given in Table 2.

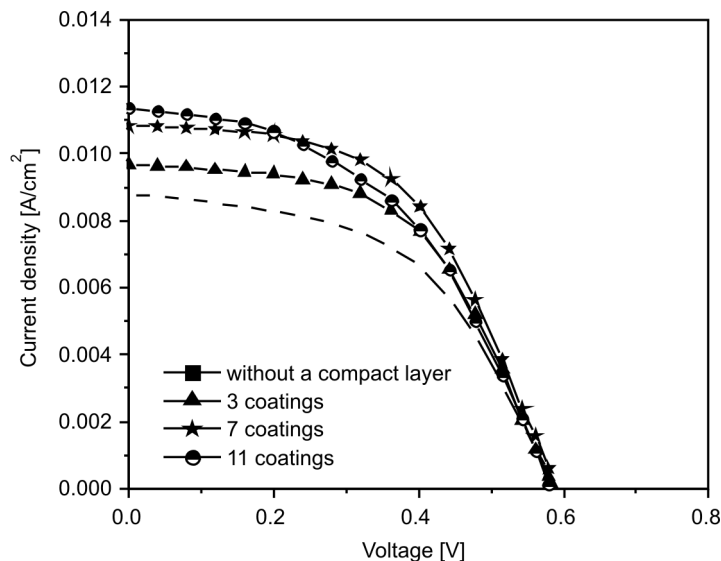


Fig. 10. J - V characteristics of a dispersed CuI solar cell with various numbers of compact layer coatings

When a ZnO compact layer was applied to cell B, the cell was found to exhibit an increase in efficiency from 2.67 to 3.38%. On applying 3 coatings of compact layer

(thickness ca. 42 nm), the efficiency increased from 2.67 to 3.06%. Efficiency was found to increase up to 3.38% with 7 numbers of coatings of compact layer corresponding to the thickness of 106 nm. With 11 coatings of compact layer (~140 nm) the efficiency decreases from 3.38% to 3.12%. At the thickness of 140 nm, the compact layer becomes thick enough to hinder the electrons from reaching the anode, which in turn worsens the performance of a solar cell [34].

Table 2. Photovoltaic parameters of DSSC with a ZnO compact layer

No. of compact layers	Thickness [nm]	J_{sc} [mA/cm ²]	V_{oc} [V]	FF	η [%]
Without layer	0	8.75	0.59	0.52	2.67
3	42±1	9.66	0.59	0.54	3.06
7	106±1	10.83	0.59	0.53	3.38
11	140±1	11.34	0.58	0.48	3.12

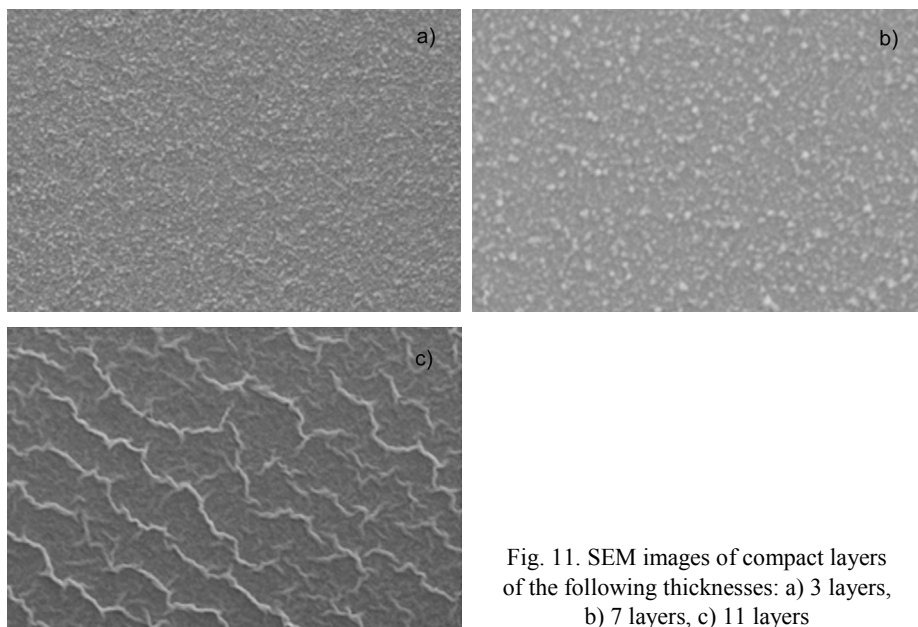


Fig. 11. SEM images of compact layers of the following thicknesses: a) 3 layers, b) 7 layers, c) 11 layers

Figure 11 shows the surface morphology (SEM images) of the compact layers 42, 106 and 140 nm thick. Uniformly tight packed grains of ZnO (Fig. 11 a, b) convert into a tetrapod-like textured surface with sharp boundaries.

4. Conclusions

Dispersion of CuI in a gel electrolyte improves the cell parameters. It is envisaged that the dispersion of CuI in the gel electrolyte results in the formation of $\text{Cu}^+/\text{I}^-/\text{I}_3^-$

complexes thereby, introducing local ordering of the redox couple. This local ordering facilitates the hole conduction towards the back electrode, thereby improving the conversion efficiency of the DSSC. Use of a ZnO compact layer in ZnO/Rose Bengal/dispersed CuI gel electrolyte cell further increases the efficiency of the solar cell, due to prevention of back transfer of electrons by blocking direct contact between the electrolyte and the conductive substrate.

Acknowledgements

This work has been financially supported under the MNRE project No. 31/7/2004-05/PV-R&D, Govt. of India. One of the authors, S.R., gratefully acknowledges the financial support in the form of JRF from UGC, New Delhi.

References

- [1] O'REGAN B., GRATZEL M., *Nature*, 353 (1991), 737.
- [2] NAZEERUDDIN M.K., KAY A., RODICIO I., HUMPHRY-BAKER R., MULLER E., LISKA P., LACHCHOPOULOS N., GRATZEL M., *J. Am. Chem. Soc.*, 115 (1993), 6382.
- [3] O'REGAN B., SCHWARTZ DANIEL T., *Chem. Mater.*, 10 (1998), 1501.
- [4] TENNAKONE K., KUMARA G.R.R.A., KUMARSINGHE A.R., WIJAYANTHA K.G.U., SIRIMANNE P.M., *Semicond. Sci. Technol.*, 10 (1995), 1689.
- [5] MURAKOSHI K., KOGURE R., YANAGIDA S., *Chem. Lett.*, 5 (1997), 471.
- [6] BACH U., WEISSORTEL F., UEBE J., GRATZEL M., SALBECK D.W., *Abstract Book, Bayreuth Polymer and Material Research Symposium, 1997*, p. 28.
- [7] MENG Q.B., TAKAHASHI K., ZHANG X.T., SUTANTO I., RAO T.N., SATO O., FUJISHIMA A., WATANABE H., NAKAMORI T., AND URAGAMI M., *Langmuir* 19 (2003), 3572.
- [8] BACH U., LUPO D., COMTE P., MOSER J.E., WEISSORTEL F., SALBECK J., SPREITZER H. & GRATZEL M., *Nature*, 395 (1998), 583.
- [9] NOGUERIA A.F., DURRANT J.R., DEPAOLI M.A., *Adv. Mater.*, 13 (2001), 826.
- [10] WANG P., ZAKEERUDDIN S.M., GRÄTZEL M., *J. Fluorine Chem.*, 125 (2004), 1241.
- [11] WANG H., LI H., XUE B., WANG Z., MENG Q., LIQUAN C., *J. Am. Chem. Soc.*, 127 (2005), 6394.
- [12] XUE B., WANG H., HU Y., LI H., WANG Z., QINGBO M., HUAN X.G., SATO O., CHEN L., FUJISHIMA A., *Photochem. Photobiol. Sci.*, 3 (2004), 918.
- [13] NAKAHARA K., TAKASU H., FONS P., YAMADA A., MATSUBARA K., HUNGER R., NIKI S., *Appl. Phys. Lett.*, 79 (2001), 4193.
- [14] RANI S., SURI P., SHISHODIA P.K., MEHRA R.M., *Solar En. Mater. Solar Cells*, 92 (2008), 1639.
- [15] KUMARA G.R.A., KANEKO S., SHIRATSUCHI K., TSUKAHARA J., TENNAKONE K., *Chem. Mater.*, 14 (2002), 954.
- [16] WANG P., ZAKEERUDDIN S.M., EXNAR I., GRATZEL M., *Chem. Commun.*, 24 (2002), 2972.
- [17] USUI H., MATSUI H., TANABE N., YANAGIDA S., *J. Photochem. Photobiol. A: Chem.*, 164 (2004), 97.
- [18] KUBO W., KITAMURA T., HANABUSA K., WADA Y., YANAGIDA S., *Chem. Commun.*, 4 (2002), 374.
- [19] WANG P., ZAKEERUDDIN S.M., EXNAR I., GRATZEL M., *J. Am. Chem. Soc.*, 125 (2003), 1166.
- [20] PRADHAN B., BATABYAL S.K., PAL A.J., *Solar En. Mater. Solar Cells* 91 (2007), 769.
- [21] DUFFY N.W., PETER L.M., RAJAPAKSE R.M.G., WIJAYANTHA K.G.U., *J. Phys. Chem. B*, 104 (2000), 8916.
- [22] MLCHIO M., SHIGEYUKI M., HIROSHI T., *Ind. Eng. Chem. Prod. Res. Dev.*, 19 (1980), 415.
- [23] GUILLENA E., CASANUEVA F., ANTA J.A., VEGA-POOT A., OSKAM G., ALCANTARA R., FERNANDEZ-LORENZO C., MARTIN-CALLEJA J., *J. Photochem. Photobiol. A: Chem.*, 200 (2008), 364.

- [24] MAJUMDER S.B., AGARWAL D.C., MOHAPATRA Y.N., KULKARNI V.N., *Integr. Ferroelectr.*, 9 (1995), 271.
- [25] GODOVSKY D., CHEN L., PETTERSSON L., INGANAS O., ANDERSSON M.R., HUMMELEN J.C., *Adv. Mater. Opt. Electron.*, 10 (2000), 47.
- [26] BEREZNEV S., KOEPPE R., KONOVALOV I., KOIS J., GUNES S., OPIK A., MELLIKOV E., SARICIFTCI N.S., *Thin Solid Films*, 515 (2007), 5759.
- [27] WEST A.R., *Solid State Chemistry and Its Application*, Wiley, New York, 1984, p. 174.
- [28] ROY M.S., BALRAJU P., MANISH K., SHARMA G.D., *Solar En. Mater. Solar Cells*, 92, (2008), 909.
- [29] SODERGREN S., HAGFELDT A., OLSSON J., LINDQUIST S.E., *J. Phys. Chem.*, 95 (1994), 5522.
- [30] BING L., PING C., CHANG-SHENG D., *Chin. J. Chem. Phys.*, 20, (2007), 816.
- [31] KANG M.-S., AHN K.-S., LEE J.-W., *J. Power Sources*, 180 (2008), 896.
- [32] STERGIOPOULOS T., ARABATZIS I.M., KATSAROS G., FALARAS A.P., *Nano Lett.*, 2 (2002), 1259.
- [33] CHEN L.-H., XUE B.-F., LIU X.-Z., LI K.-X., LUO Y.-H., MENG Q.-B., WANG R.-L., CHEN L.-Q., *Chin. Phys. Lett.*, 2 (2007), 555.
- [34] BIN P., JUNGSMANN G., JAGER C., HAARER D., SCHMIDT H.W., THELAKKAT M., *Coord. Chem. Rev.*, 248 (2004), 1479.

Received 18 December 2008

Revised 10 July 2009